DOI: 10.1002/anie.200905497

Self-Assembly

Hierarchical Self-Assembly of a Chiral Metal–Organic Framework Displaying Pronounced Porosity**

*Jack K. Clegg, Simon S. Iremonger, Michael J. Hayter, Peter D. Southon, René B. Macquart, Martin B. Duriska, Paul Jensen, Peter Turner, Katrina A. Jolliffe, Cameron J. Kepert, George V. Meehan, and Leonard F. Lindoy**

Significant recent attention has been devoted to the development of useful self-assembled hybrid materials.[1] This is particularly the case for metal–organic frameworks (MOFs), which display properties such as regularity, porosity, robustness, and high surface area that lead to potential applications in areas such as catalysis, gas separation, and storage.[2,3] Our research groups and others have been developing new methods for the synthesis of both discrete and extended metal–organic materials, with particular interest in the controlled generation of increased structural complexity.[4] Herein we report a hierarchical self-assembly strategy which has been used to synthesize a new metal–organic framework. This strategy differs from the commonly employed molecular building block (MBB) and secondary building unit (SBU) approaches, where single metal ions or small inorganic clusters (polyhedra) are linked by bridging (often carboxylate) ligands in a one-pot reaction.[5] In these approaches, substantial pore volume is achieved principally through the enthalpically favorable formation of an open framework overcoming the entropic penalties associated with the entrapment of solvent guest molecules. Kinetic control over the formation of the framework is achieved largely through the trial-and-error optimization of synthetic conditions to prevent formation of unwanted kinetic intermediates.[6]

In the hierarchical approach used here we have employed a series of distinct self-assembly steps, which operate across different levels of complexity, to incorporate predesigned, kinetically stable, discrete neutral supramolecular components into a metal–organic framework. In this way we show that it is possible to transcribe the properties of the discrete subcomponent into those of the framework product. This method involves the initial design and assembly of a discrete two-dimensional (2D) void-containing tecton containing unsaturated metal centers, followed by linkage of these sites with a bridging group in such a way that it is possible to transform the 2D voids in the subcomponent into 3D voids in a framework material. By using this approach we have generated a new neutral chiral MOF that displays significant porosity and gas-sorption behavior, and hence demonstrate that the host–guest properties of our discrete building blocks can be successfully imparted to the final MOF.

Building on our well-established methods for assembling metallosystems incorporating β-diketone ligands,[7,8] we constructed the large discrete triangular subcomponent $[Cu_3L_3]$. This moiety is relatively unusual among discrete systems of this type in that it contains coordinatively unsaturated metal centers in combination with a large void area—both useful attributes for the formation of a MOF with significant porosity.

H_2L (Scheme 1) was synthesized by a Claisen condensation between dimethyl biphenyl-4,4′-dicarboxylate and 3,3-dimethylbutan-2-one (the synthesis and characterization of H_2L is given in the Supporting Information). The target complex $[Cu_3L_3]\cdot H_2O$ was formed in 80% yield after slow addition of copper(II) chloride to a solution of the ligand in THF in the presence of Na_2CO_3. Microanalysis confirmed the above stoichiometry, and the product was assigned a triangular structure by analogy with related smaller trinuclear copper complexes previously described by us and others.[8,9] This assignment was supported by the results of a single-crystal X-ray diffraction analysis of the closely related Co^{II} complex[10] $[Co_3L_3(py)_6]\cdot 5.55\,py\cdot 0.6\,H_2O$ (py = pyridine). This product has the expected discrete triangular structure (Figure 1; see also Figure S5 in the Supporting Information) in which three L ligands bridge three Co^{II} ions, such that L forms the side of a neutral, essentially equilateral triangle with sides of about 15 Å. Each Co^{II} center is six coordinate with a pseudooctahedral coordination geometry; the axial coordination sites are occupied by the pyridine coligands. Indeed, this trinuclear

[*] Dr. J. K. Clegg, Dr. S. S. Iremonger, M. J. Hayter, Dr. P. D. Southon, Dr. R. B. Macquart, Dr. P. Jensen, Dr. P. Turner, Prof. K. A. Jolliffe, Prof. C. J. Kepert, Prof. L. F. Lindoy
School of Chemistry, F11, The University of Sydney
Sydney, NSW 2006 (Australia)
Fax: (+61) 2-9351-3329
E-mail: lindoy@chem.usyd.edu.au
Prof. G. V. Meehan
School of Pharmacy and Molecular Sciences, James Cook University
Douglas, Townsville, Qld 4814 (Australia)
Dr. M. B. Duriska
School of Chemistry, Monash University
Clayton, Vic 3800 (Australia)

[**] Use of the ChemMatCARS Sector 15 at the Advanced Photon Source was supported by the Australian Synchrotron Research Program, which is funded by the Commonwealth of Australia under the Major National Research Facilities Program. ChemMatCARS Sector 15 is also supported by the National Science Foundation/Department of Energy under grant numbers HE9522232 and CHE0087817, and by the Illinois board of higher education. The Advanced Photon Source is supported by the US Department of Energy, Basic Energy Sciences, Office of Science, under contract no. W-31-109-Eng-38.

Supporting information for this article is available on the WWW under http://dx.doi.org/10.1002/anie.200905497.

 © 2010 Wiley-VCH Verlag GmbH & Co. KGaA, Weinheim

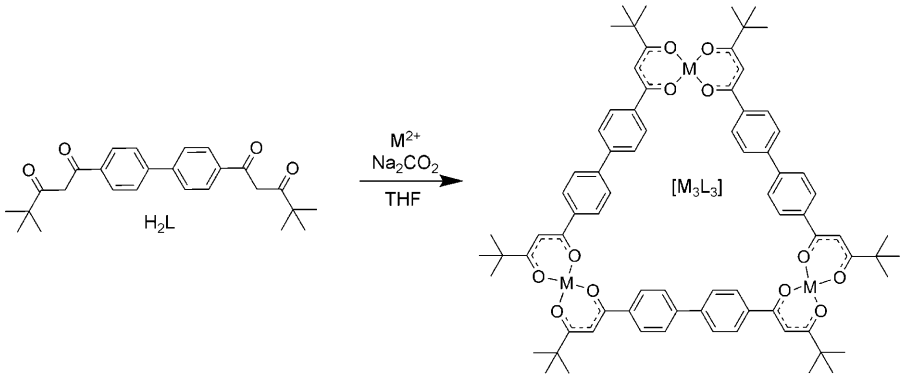

Scheme 1. Generation of a trinuclear triangle M_3L_3 from H_2L and a divalent metal ion.

bound to these metal centers on one face of the mean plane of the triangle. The structure crystallizes in the chiral cubic space group $P2_13$ and there is one third of a triangular $[Cu_3L_3]$ entity in the asymmetric unit. Overall, the structure adopts a highly distorted (10,3)-a topology, in which each of the triangular and hmt units act as trigonal linking components.

The framework houses substantial pore volume, which consists of large extended pyramidal voids (9.4 Å diameter) linked by a three-

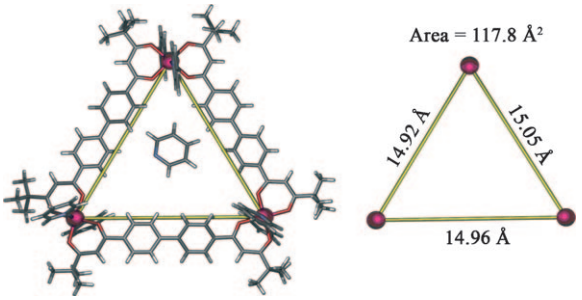

Figure 1. Schematic representation of the crystal structure of $[Co_3L_3(py)_6]\cdot 5.55\,py\cdot 0.6\,H_2O$. Solvate molecules not shown.

Co^{II} species ranks amongst the largest neutral $M_3L'_3$ triangles so far characterized structurally.[11] The area enclosed by the metal centers in this species, at about 118 $Å^2$, is of sufficient size to allow solvent, including pyridine (used for its preparation), to occupy the void; a disordered pyridine guest molecule occupies the cavity in the solid-state structure. This large void area contrasts with the much smaller void of approximately 48 $Å^2$ present in the smaller related trinuclear triangles.[8,9]

After the synthesis of the $[Cu_3L_3]\cdot H_2O$ subcomponent, the next step in the hierarchical assembly was the reaction of this species with a suitable linking ligand to form a MOF. Hexamethylenetetramine (hmt) was chosen for this reaction since it had previously been shown to act as a three-connecting ligand, and it was hence anticipated that it was likely to generate a three-dimensional framework upon reaction with $[Cu_3L_3]\cdot H_2O$.

The addition of a hot solution of hmt in THF to $[Cu_3L_3]\cdot H_2O$ dissolved in a hot solution of THF resulted in the formation of small dark-green prismatic crystals. Microanalysis of these crystals after drying under a vacuum gave a $[Cu_3L_3]$/hmt ratio of 1:1. The crystal structure also confirmed this stoichiometry, and showed a neutral 3D network in which both hmt and $[Cu_3L_3]$ are present as triply bridging units that lead to an overall formula of $[Cu_3L_3(hmt)]_n$. The structural fragment shown in Figure 2 has a threefold axis passing through the unbound nitrogen atom of the hmt unit to give a propeller-like arrangement. Each $[Cu_3L_3]$ unit incorporates three five-coordinate Cu^{II} centers, with three hmt linkers

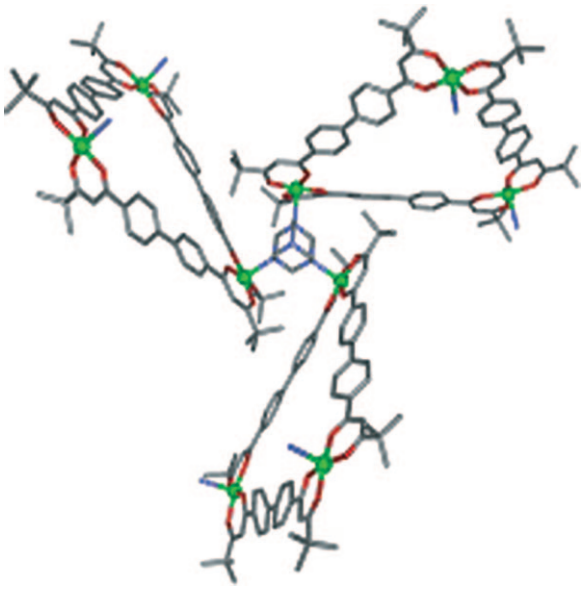

Figure 2. Schematic representation of the arrangement of three $[Cu_3L_3]$ units around an hmt linker in the crystal structure of $[Cu_3L_3(hmt)]_n$.

dimensional network of very narrow pores (3.9 Å diameter). The use of the SQUEEZE function of PLATON[12] to estimate the volume and contents of these pores showed the pore volume to be approximately 56% of the total volume of the unit cell. No ordered residual solvent was observed in the difference Fourier map (largest residual Q peak 1.12 $e^-\,Å^{-3}$) within these pores. Nevertheless, the residual electron count was 3698 e^- per unit cell, which corresponds to the equivalent of 90 THF molecules. A thermogravimetric analysis was in agreement with this occupancy, where a 17.5% weight loss was observed by 375 K (ramp rate 1 K min^{-1}), after which no further change in weight was observed until 500 K. In contrast, a second thermogravimetric analysis of a sample after vacuum drying indicated that the sample was significantly desolvated before the analysis was commenced. In this case a weight loss of 8.75% was obtained by 500 K. A powder diffraction pattern of a finely ground vacuum-dried sample indicated a significant change in the unit-cell dimensions, with the refined cubic unit-cell length decreasing from 24.2236(11) Å in the single-crystal analysis to 20.863(5) Å

 © 2010 Wiley-VCH Verlag GmbH & Co. KGaA, Weinheim

(Figure S4 in the Supporting Information), thus indicating that the network contracts significantly upon desolvation.

A proof-of-concept study was subsequently undertaken on a bulk sample of the desorbed apohost material $[Cu_3L_3(hmt)]_n$ to determine if it might be a suitable candidate for the adsorption of solvents or gases into its pores, despite the observed contraction of the framework upon desorption of THF. The N_2 sorption isotherm of $[Cu_3L_3(hmt)]_n$ at 77 K is shown in Figure 3. Overall the adsorption is atypical, with

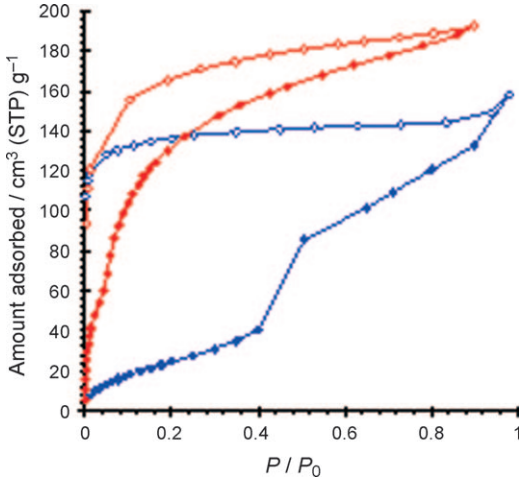

Figure 3. The sorption isotherms for N_2 at 77 K (blue) and Ar at 87 K (red) in desolvated $[Cu_3L_3(hmt)]_n$ (adsorption closed diamond, desorption open). See also Figures S1 and S3 in the Supporting Information. STP = standard temperature and pressure.

pronounced hysteresis and a significant step at $0.4\,P/P_0$ attributable to the activated transport of N_2 (dimensions $3.054 \times 2.991 \times 4.046$ Å) through narrow pore windows.[12] The size of these windows are presumably reduced further in the desolvated apohost framework, and also possibly as a result of some distortion of the bulk framework accompanying N_2 sorption. Under such conditions, the diffusion barrier requires activation energy for the molecules to force their way through the narrow pore to access the larger voids. The abrupt adsorption at $0.4\,P/P_0$ represents the "break-through" point, where sufficient back pressure exists to overcome the diffusion barrier and allow saturation of the pores. To explore this process further the Ar sorption isotherm was measured at 87 K. As Ar (3.4 Å) is smaller than N_2, and 87 K corresponds to a greater thermal energy of both the host and guest, it would be expected that the adsorption of Ar would be less restricted than for the N_2 case. Indeed, significantly less hysteresis is observed in the Ar isotherm than in the case of N_2, and the adsorption isotherm is also more abrupt. Below $0.4\,P/P_0$, the adsorption of Ar is about five times greater than that of N_2, thus indicating the potential for use in selective separation applications.

H_2 sorption isotherms were measured at 77 and 87 K and are shown in the Supporting Information (Figure S2). A modest adsorption of 0.6 wt% occurs at 77 K and 1.15 bar, with saturation not reached at this point. Only a small degree of hysteresis is observed. As H_2 is smaller than both N_2 and Ar, this is in keeping with the proposed mechanism discussed above. The enthalpy of adsorption (ΔH_{ads}) at zero loading was calculated to be 8.0 kJ mol^{-1}, which is higher than that for typical van der Waals type interactions (4–6 kJ mol^{-1}) seen in most MOFs.[3] The comparatively high ΔH_{ads} value likely arises from a combination of the interaction of dihydrogen with the coordinatively unsaturated Cu^{II} sites and multiple interactions resulting from the presence of small pores.

The present hierarchical synthetic approach involving the initial assembly of a cavity-containing metallotriangle with accessible binding sites followed by linkage with a trifunctional amine bridging group has proved successful both in achieving considerable structural complexity and in transcribing the 2D voids in the component triangle into 3D voids in the framework product. This result points the way to the future use of hierarchical strategies for the generation of new porous frameworks of this type, through which sophisticated control of the thermodynamics and kinetics of the assembly process may be achieved and the specific aspects of the framework precursors (in this case of a host–guest nature) exploited. This approach, which mirrors that taken by nature in the formation of many highly sophisticated biomolecular architectures including the assembly of proteins, nucleic acids, and virus capsids, may in principle be used to obtain complex metastable frameworks of very considerable complexity. In the present case, the product is an unusual chiral 3D framework. Gas sorption measurements have shown this thermally robust framework to support significant void volume, with the adsorption behavior rationalized in terms of the presence of large pores connected by narrow windows—a result that adds to our general understanding of structure/function relationships within this category of potentially industrially and environmentally important materials.

Experimental Section

All reagents and solvents were purchased from commercial sources. Tetrahydrofuran was predried over sodium wire before use. UV/Vis solid-state spectra were recorded on a Cary 1E spectrophotometer. TGA analysis was performed using a TA instruments HI-Res TGA2850 thermogravimetric analyser under a nitrogen gas atmosphere.

$[Co_3L_3(py)_6]\cdot 5.55\,py\cdot 0.6\,H_2O$: A warm solution of H_2L (0.203 g, 0.5 mmol) in pyridine (10 mL) was added to a warm solution of cobalt(II) acetate tetrahydrate (0.125 g, 0.5 mmol) in pyridine (5 mL). The solution was stirred, filtered, and then allowed to evaporate slowly; crystals of the product formed after several days. On removal of the complex from the mother liquor it rapidly loses both the pyridine solvate as well as the coordinated pyridine ligands. One of the above crystals was used directly in the crystallographic studies. The elemental analysis of a sample of this product that had been dried under vacuum then stored in air corresponded to a product in which some of the pyridine molecules had been lost and replaced by water molecules, $[Co_3L_3]\cdot(C_5H_5N)_{0.25}\cdot 2.5\,H_2O$. Elemental analysis (%) calcd for $C_{78}H_{84}Co_3O_{12}\cdot(C_5H_5N)_{0.25}\cdot 2.5\,H_2O$: C 65.39, H 6.25, N 0.24; found: C 65.41, H 6.61, N 0.25.

$[Cu_3L_3]\cdot H_2O$: A solution of H_2L (0.162 g, 0.4 mmol) in dry tetrahydrofuran (40 mL) was added to excess Na_2CO_3 (ca. 1.0 g, 0.01 mol) suspended in dry THF (10 mL). This mixture was stirred for 1 h before copper(II) chloride dihydrate (0.068 g, 0.4 mmol) in tetrahydrofuran (40 mL) was added dropwise. The mixture was then stirred at 40 °C for 16 h before filtering the resulting clear

 © 2010 Wiley-VCH Verlag GmbH & Co. KGaA, Weinheim

solution. The solvent was then reduced to a small volume on a rotary evaporator to yield the solid complex as a microcrystalline powder, which was collected by filtration and washed with cold acetonitrile (20 mL) followed by diethyl ether (20 mL). The sample was then crushed and dried under vacuum over P_2O_5. Yield 0.151 g (80 %), green microcrystalline powder. Elemental analysis (%) calcd for $C_{78}H_{84}Cu_3O_{12}\cdot H_2O$: C 65.94, H 6.11; found: C 65.79, H 6.18, N 0.25. UV/Vis (solid state): 420, 504, 684, 824 nm.

$[Cu_3L_3(hmt)]_n$: A solution of hexamethylenetetramine (0.014 g, 0.1 mmol) in warm THF (20 mL) was added to a warm stirred solution of $[Cu_3L_3]\cdot H_2O$ (0.142 g, 0.1 mmol) in THF (40 mL). The mixture was brought to reflux before cooling to room temperature and subsequent filtration. Slow evaporation of the filtrate resulted in the formation of crystals suitable for X-ray analysis. Samples for microanalysis and gas-sorption studies were collected by vacuum filtration, washed with cold THF (20 mL), and then dried under vacuum. The sample was then crushed, washed with diethyl ether, and dried under vacuum. Yield 95 % (0.156 g). Elemental analysis (%) calcd for $C_{84}H_{84}Cu_3N_4O_{12}\cdot H_2O$: C 64.64, H 6.33, N 3.59; found: C 64.60, H 6.49, N 3.61. UV/Vis (solid state): 521, 646, 795 nm.

The Supporting Information contains additional experimental details of the ligand synthesis, X-ray data, and adsorption measurements. CCDC 748269 ($[Co_3L_3(py)_6]\cdot 5.55\,py\cdot 0.6\,H_2O$) and 748270 ($[Cu_3L_3(hmt)]$) contain the supplementary crystallographic data for this paper. These data can be obtained free of charge from The Cambridge Crystallographic Data Centre via www.ccdc.cam.ac.uk/data_request/cif.

Received: September 30, 2009
Published online: January 7, 2010

Keywords: adsorption · coordination modes · self-assembly · supramolecular chemistry

[1] a) P. Mal, B. Breiner, K. Rissanen, J. R. Nitschke, *Science* **2009**, *324*, 1697 – 1699; b) R. M. Capito, H. S. Azevedo, Y. S. Velichko, A. Mata, S. I. Stupp, *Science* **2008**, *319*, 1812 – 1816; c) C. J. Kepert, *Chem. Commun.* **2006**, 695 – 700.

[2] a) L. J. Murray, M. Dincă, J. R. Long, *Chem. Soc. Rev.* **2009**, *38*, 1294 – 1314; b) J.-Y Lee, O. K. Farha, J. Roberts, K. A. Scheidt, S.-B. T. Nguyen, J. T. Hupp, *Chem. Soc. Rev.* **2009**, *38*, 1450 – 1459; K. M. Thomas, *Dalton Trans.* **2009**, 1487 – 1505; Z. Wang, G. Chen, K. Ding, *Chem. Rev.* **2009**, *109*, 322 – 359.

[3] a) J.-R. Li, R. J. Kuppler, H.-C. Zhou, *Chem. Soc. Rev.* **2009**, *38*, 1477 – 1504; b) D. Farrusseng, S. Aguado, C. Pinel, *Angew. Chem.* **2009**, *121*, 7638 – 7649; *Angew. Chem. Int. Ed.* **2009**, *48*, 7502 – 7513.

[4] a) M. B. Duriska, S. M. Neville, B. Moubaraki, J. D. Cashion, G. J. Halder, K. W. Chapman, C. Balde J.-F. Létard, K. S. Murray, C. J. Kepert, S. R. Batten, *Angew. Chem.* **2009**, *121*, 2587 – 2590; *Angew. Chem. Int. Ed.* **2009**, *48*, 2549 – 2552; b) M. B. Duriska, S. M. Neville, J. Lu, S. S. Iremonger, J. F. Boas, C. J. Kepert, S. R. Batten, *Angew. Chem.* **2009**, *121*, 9081 – 9084; *Angew. Chem. Int. Ed.* **2009**, *48*, 8919 – 8922.

[5] a) J. J. Perry IV, J. A. Perman, M. J. Zaworotko, *Chem. Soc. Rev.* **2009**, *38*, 1400 – 1417; b) D. J. Tranchemontagne, J. L. Mendoza-Cortés, M. O'Keeffe, O. M. Yaghi, *Chem. Soc. Rev.* **2009**, *38*, 1257 – 1283; c) D. F. Sava, V. C. Kravtsov, J. Eckert, J. F. Eubank, F. Nouar, M. Eddaoudi, *J. Am. Chem. Soc.* **2009**, *131*, 10394 – 10396; d) G. J. Halder, C. J. Kepert, B Moubaraki, K. S. Murray, J. D. Cashion, *Science* **2002**, *298*, 1762 – 1765; e) Q. Li, W. Zhang, O. Š. Miljaní, C.-H. Sue, Y.-L. Zhao, L. Liu, C. B. Knobler, J. F. Stoddart, O. M. Yaghi, *Science* **2009**, *325*, 855 – 859.

[6] S. Hausdorf, J. Wagler, R. Mossig, F. O. R. L. Mertens, *J. Phys. Chem. A* **2008**, *112*, 7567 – 7576.

[7] a) J. K. Clegg, L. F. Lindoy, J. C. McMurtrie, D. Schilter, *Dalton Trans.* **2005**, 857 – 864; b) J. K. Clegg, K. Gloe, M. J. Hayter, O. Kataeva, L. F. Lindoy, B. Moubaraki, J. C. McMurtrie, K. S. Murray, D. Schilter, *Dalton Trans.* **2006**, 3977 – 3984; c) J. K. Clegg, *Aust. J. Chem.* **2006**, *59*, 660; d) D. J. Bray, J. K. Clegg, L. F. Lindoy, D. Schilter, *Adv. Inorg. Chem.* **2006**, *59*, 1 – 37; e) J. K. Clegg, D. J. Bray, K. Gloe, K. Gloe, M. J. Hayter, K. A. Jolliffe, G. A. Lawrance, G. V. Meehan, J. C. McMurtrie, L. F. Lindoy, M. Wenzel, *Dalton Trans.* **2007**, 1719 – 1730; f) F. Li, J. K. Clegg, P. Jensen, K. Fisher, G. V. Meehan, L. F. Lindoy, *Angew. Chem.* **2009**, *121*, 7193 – 7197; *Angew. Chem. Int. Ed.* **2009**, *48*, 7059 – 7063.

[8] a) J. K. Clegg, L. F. Lindoy, B. Moubaraki, K. S. Murray, J. C. McMurtrie, *Dalton Trans.* **2004**, 2417 – 2422; b) J. K. Clegg, L. F. Lindoy, J. C. McMurtrie, D. Schilter, *Dalton Trans.* **2006**, 3114 – 3121; c) J. K. Clegg, D. J. Bray, K. Gloe, K. Gloe, K. A. Jolliffe, G. A. Lawrance, L. F. Lindoy, G. V. Meehan, M. Wenzel, *Dalton Trans.* **2008**, 1331 – 1340; d) D. J. Bray, B. Antonioli, J. K. Clegg, K. Gloe, K. Gloe, K. A. Jolliffe, L. F. Lindoy, G. Wei, M. Wenzel, *Dalton Trans.* **2008**, 1683 – 1685.

[9] D. V. Soldatov, A. S. Zanina, G. D. Enright, C. I. Ratcliffe, J. A. Ripmeester, *Cryst. Growth Des.* **2003**, *3*, 1005 – 1013.

[10] See the Supporting Information for details of the structural characterization.

[11] E. Zangrando, M. Casanova, E. Alessio, *Chem. Rev.* **2008**, *108*, 4979 – 5013.

[12] A. L. Spek, *J. Appl. Crystallogr.* **2003**, *36*, 7 – 13.

[13] C. E. Webster, R. S. Drago, M. C. Zerner, *J. Am. Chem. Soc.* **1998**, *120*, 5509 – 5516.

[14] a) T. X. Nguyen, S. K. Bhatia, *J. Phys. Chem. C* **2007**, *111*, 2212 – 2222; b) H. Kim, D. G. Samsonenko, M. Yoon, J. W. Yoon, Y. K. Hwang, J.-S. Chang, K. Kim, *Chem. Commun.* **2008**, 4697 – 4699.

 © 2010 Wiley-VCH Verlag GmbH & Co. KGaA, Weinheim